Gesellschaft für Anlagen- und Reaktorsicherheit (GRS) mbH

Ventilation Test at Mont Terri: Geoelectric Monitoring of the Opalinus Clay Desaturation

Phase 2

GRS - 235

Gesellschaft für Anlagen- und Reaktorsicherheit (GRS) mbH

Ventilation Test at Mont Terri: Geoelectric Monitoring of the Opalinus Clay Desaturation

Phase 2

Klaus Wieczorek
Chun-Liang Zhang
Tilmann Rothfuchs

April 2008

Remark:

This report was prepared under contract No. 02 E 9914 with the Bundesministerium für Wirtschaft und Technologie (BMWi) and under contract No. F16W-CT-2003-02389 with the European Commission.

The work was conducted by the Gesellschaft für Anlagen- und Reaktorsicherheit (GRS) mbH.

The authors are responsible for the content of this report.

GRS - 235
ISBN 978-3-939355-09-0

Deskriptoren:
Endlagerung, EU, Gestein, Geoelektrik, Geomechanik, Internationale Zusammenarbeit, Labor, Meßprogramm, Schweiz, Tomographie, Überwachung

Table of Contents

1 Introduction

Between December 2001 and May 2004, a ventilation experiment (VE) was performed in the Mont Terri Underground Research Laboratory (URL) and co-financed by the Commission of the European Communities under contract No. FIKW-CT-2001-00126. The objective was to investigate the desaturation of consolidated clay formations in consequence of the ventilation of underground openings of a repository in such a formation. A microtunnel of 1.3 m diameter was excavated and sealed off (Figure 1-1). A ventilation system was installed and a test section of 10 m length was extensively instrumented (Figure 1-2).

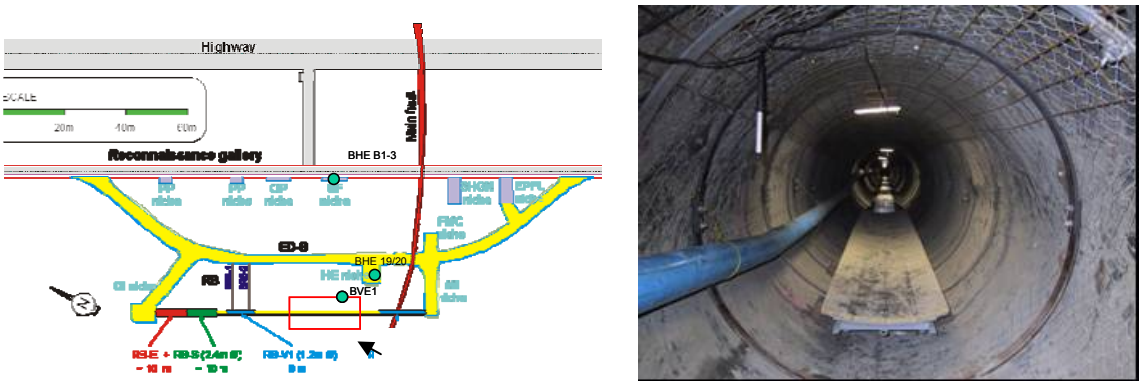

a) Position of VE test section in the URL b) View into the microtunnel

Figure 1-1 Microtunnel at the Mt. Terri Underground Research Laboratory

GRS' task in the frame of the project was the monitoring of saturation changes in the rock mass adjacent to the microtunnel by means of geoelectric tomography. For this aim, an electrode array was installed in section SE in the microtunnel (see Figure 1-2). In the geoelectric measurements advantage is taken of the dependence of the electric resistivity of materials on the water (solution) content. With the tomographic measurements the resistivity distribution in a portion of rock is determined and can then be interpreted in terms of solution content distribution.

The results of the geoelectric measurements in this phase 1 of the VE-experiment are reported in detail in /ROT 04/.

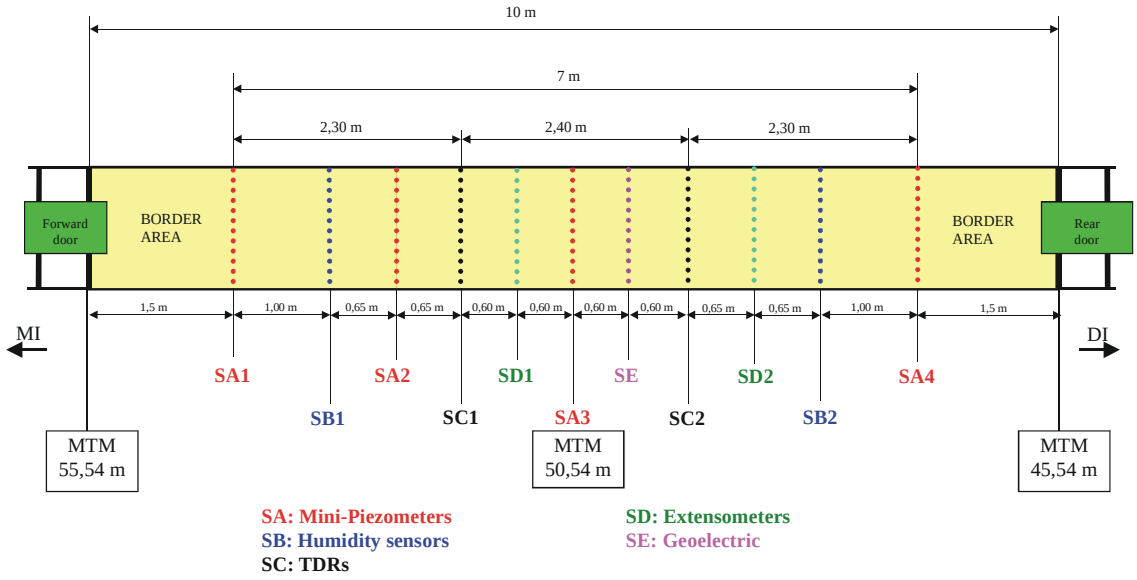

Figure 1-2 Instrumented VE test section in the microtunnel at the Mt. Terri URL

In the course of this first phase of the VE-experiment it was decided to continue the experiment in a second phase and to include this part of the experiment in the Integrated EC Project "Nearfield Processes (NF-PRO)".

In addition to the geoelectric measurements, the NF-PRO work programme comprised also laboratory ventilation experiments and related model simulations in order to support the correct interpretation of de- and resaturation effects observed in situ in the argillaceous rock.

2 Geoelectric in-situ monitoring

In the following sections, the measurement and evaluation technique, the instrumentation, and the results obtained in the second phase of the VE are described.

2.1 Measuring Techniques

The technique most frequently applied for geoelectric measurements in the field is the four-point method (Figure 2-1). An electric direct current (DC) is supplied to the formation via two electrodes. The magnitude and direction of the resulting electric field are dependent on the conductivity conditions in the rock. The potential difference between two other electrodes is measured. The input electrodes (C_1, C_2) and the output electrodes (P_1, P_2) are arranged as single dipoles (Figure 3-3). For a medium with spatially constant electric resistivity, the resulting potential difference ΔV is given by Ohm's law (Equation 1), so that the resistivity ρ can be derived from a single measurement.

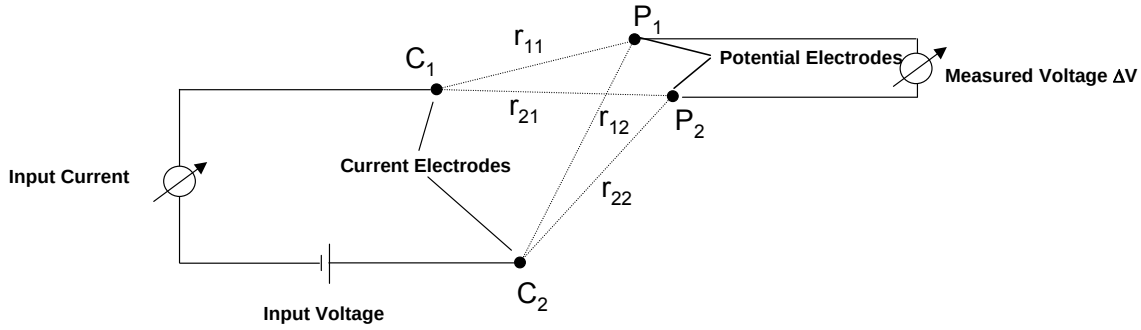

Figure 2-1 Principle configuration of a dipole-dipole measurement

$$\Delta V = \frac{1}{4\pi} I\rho \left(\frac{1}{r_{11}} - \frac{1}{r_{12}} - \frac{1}{r_{21}} + \frac{1}{r_{22}}\right) \tag{2.1}$$

In the normal case of a spatially varying resistivity, the resistivity obtained by evaluating Equation 2.1 for a single measurement is an apparent resistivity. A large number of measurements with different current and potential dipoles is required to reconstruct the underlying resistivity distribution (see next section). For a complete data set, the position of the input dipole is fixed and the output dipole is moved around the area to

be investigated. Afterwards, the input dipole is moved to another position, and the measurements are repeated.

Although methods of DC geoelectrics are employed for the evaluation of the measurements, modern geoelectric systems use low-frequency alternating current (AC) rather than direct current. The reasons are:

- Direct current would cause electrolytic polarization, i. e., concentration of ions around the electrodes. This is prevented by periodic reversal of the current.
- Telluric currents, i. e., natural electric currents in the ground, can be accounted for in the measurements when the current is reversed and the measurement results are averaged, since the telluric currents do not change their polarity.

2.2 Measurement Evaluation

Measurement evaluation is performed by inverse finite element modelling. Starting with a usually homogeneous model, the expected vector of apparent resistivities for the set of measurement configurations is calculated and compared to the actually measured apparent resistivities. The model is then iteratively improved in order to minimize the deviations between calculated and measured values.

The finite element mesh has to be adapted to the electrode array. The maximum attainable resolution is half the electrode spacing; this is the minimum side length of the finite elements. On the other hand, the attainable resolution has to be considered when designing the electrode array. Half the electrode spacing is the theoretically maximum attainable resolution – if an electrode was placed at every second grid point of the mesh, the inversion result would be definite. In reality, such a high number of electrodes and related measurement configurations is not feasible. Consequently, there are areas further away from electrodes where resolution and accuracy decrease. Therefore, scoping calculations were performed during the first phase of the VE in order to find out whether the expected effects could be detected /ROT 04/.

For the evaluation of the measurements, GRS uses the commercial software package SensInv2D /FEC 01/ which allows a two-dimensional inversion of the measured apparent resistivity data. Several strategies for applying iterative improvements to the resistivity model are implemented in this software. GRS employs the multiplicative

simultaneous inversion reconstruction technique (MSIRT) /KEM 95/ which is controlled by the sensitivity distribution of the model.

Evaluation of the geoelectric measurements leads to a two-dimensional resistivity distribution that is supposed to be close to the true resistivity field. In order to interpret this resistivity distribution in terms of water content distribution, laboratory measurements have been performed at defined saturation conditions in the first phase of the VE (see Section 2.4). Using the results of the laboratory calibrations, information on water content can be derived from the resistivity distribution.

2.3 Measuring Array and Monitoring System

The measuring array consists of four electrode chains which are installed in 1 m deep boreholes drilled in a plane perpendicular to the microtunnel axis. The boreholes reach radially away from the microtunnel and are arranged in one quarter section (Figure 2-2). The spacing of the electrodes in the boreholes is 5 cm to allow a maximum resolution of resistivity distribution of about 2.5 cm. 80 electrodes were installed in the four boreholes and 19 additional electrodes on the microtunnel wall within the selected quarter section. The complete array consists of 99 electrodes.

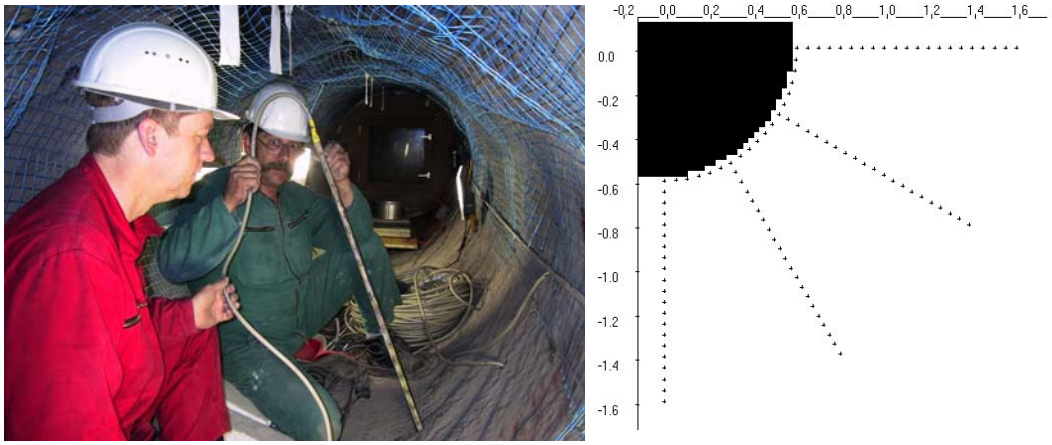

a) Installation of an electrode chain b) layout of complete electrode array

Figure 2-2 Geoelectric array around the VE microtunnel

The electrodes had been installed in the first phase of the VE, after the first desaturation phase, however, the coupling of the borehole electrodes had become

insufficient. Therefore, the borehole electrodes were withdrawn and newly installed. Instead of filling the remaining volume of the borehole with rock powder and compacting the rock powder as far as achievable by stamping with a stick, which was the procedure in the first phase, a spring coupling was provided using a rubber tube. This action was successful – the electrode coupling remained satisfying throughout the whole project.

The RESECS system is a PC-controlled DC-resistivity monitoring system for high resolution tomography and other geoelectric applications. It consists essentially of the following components:

- Resistivity meter and embedded PC
- Electrode decoder array
- Uninterruptable power supply

The resistivity meter and the embedded PC as well as the decoder array boxes are integrated in waterproof and dust-proof compact military standard housings. The complete encapsulation of the system was considered necessary because of significant dust development usually occurring during drilling campaigns at Mont Terri URL.

The RESECS measuring software runs under MSWindows98. All input of measuring parameters is menu-driven. The system offers the possibility to create standard configurations like Wenner, Schlumberger, Dipole-Dipole as well as user defined configurations. A detailed description of the monitoring system is given in the final report of the VE phase 1 /ROT 04/.

The measurements run fully automatic once per day. A total of 3543 single configurations make up one dataset. The data are transferred regularly to Braunschweig via telephone line.

2.4 Laboratory Calibration

For the interpretation of the geoelectric in-situ measurements performed during the Ventilation Experiment (VE) in the Mont Terri URL, laboratory calibrations were carried out in the GRS laboratory in Braunschweig in order to determine the relation between

electric resistivity and the water content of the Opalinus Clay. This was done during the phase 1 of the VE. A short summary of the results is given in this section; a detailed discussion of the measurements can be found in the phase 1 final report /ROT 04/.

The principle of the calibration measurements was to determine the resistivity of a sample as a function of the sample's saturation using a standard four-point configuration. Two methods were used to vary the sample saturation:

First, the samples were investigated at the state of delivery without any additional saturation in order to determine the initial resistivity of a sample. Resistivities at lower water content were then determined by drying at ambient conditions.

Afterwards, the samples were saturated. Starting from the state of full saturation, the water content of the samples was reduced by different steps: First by drying at ambient temperature, then under vacuum, and later also by heating. At each stage of drying or saturation, the resistivities were measured, respectively. Because the water content w is given by the individual wet mass in relation to the dry mass, the samples were finally dried at 105 °C to constancy of mass which is assumed to represent the completely dry mass. The actual water content was then calculated on basis of the actual mass reduction during the individual drying steps under consideration of the initial water content.

The combination of the results of all measurements is shown in Figure 2-3. In spite of the different procedures, the results are quite comparable. Obviously, the saturation procedure had no influence on the behaviour of the samples. The measurements at comparable water contents are repeatable.

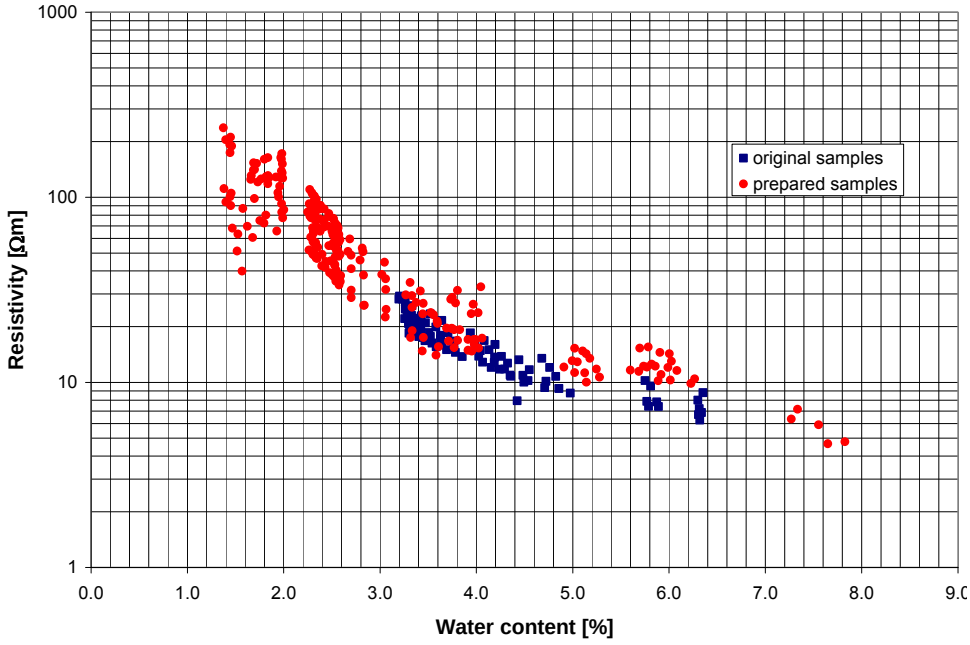

Figure 2-3 Combination of the results of the resistivity measurements after saturation and drying, and at the state of delivery without additional saturation

2.5 Measurement Results and Interpretation

2.5.1 Summary of the first phase of VE

The first phase of the Ventilation Test lasted from December 2001 until May 2004. The geoelectric measurements were started in September 2002. During a first resaturation phase, the resistivities obtained ranged first between 6 to 25 Ωm and reduced to 2.5 to 15 Ωm which can be related to almost fully saturated clay rock.

In the beginning of July 2003, ventilation with 30 % of humidity followed the resaturation phase. Since September 4, 2003 the microtunnel was ventilated with 0 to 20 % air humidity. The first desaturation phase lasted until January 25, 2004. A gradual resistivity increase in a zone of 40 to 50 cm width around the microtunnel was detected during this time. Saturation decreased to about 50 % in the vicinity of the microtunnel until this date. Further details can be found in /ROT 04/.

2.5.2 Second resaturation phase

The first desaturation phase was followed by another resaturation phase. Reliable geoelectric measurements could, however, only be performed after the re-installation of electrodes in September 2004. By then, the rock was already widely saturated, as can be taken from Figure 2-4 which shows a rather uniform resistivity distribution below 10 Ωm.

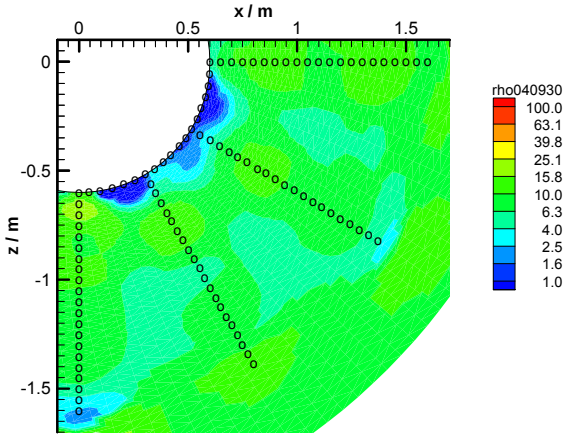

Figure 2-4 Resistivity tomogram of September 30, 2004

A somewhat lower resistivity close to the tunnel wall may be caused by an increased ion concentration of the pore solution due to the previous drying or to an increased porosity and thus higher pore solution content at full saturation in the excavation damaged zone. No significant changes in the resisitivity distribution were found until the end of June, 2005.

2.5.3 Second desaturation phase

A second desaturation phase was started on July 11, 2005 with ventilation with dry air at a flow rate of 60 m^3/h and lasted until December 21, 2006. Figure 2-5 shows the gradual resistivity increase close to the tunnel wall during this time.

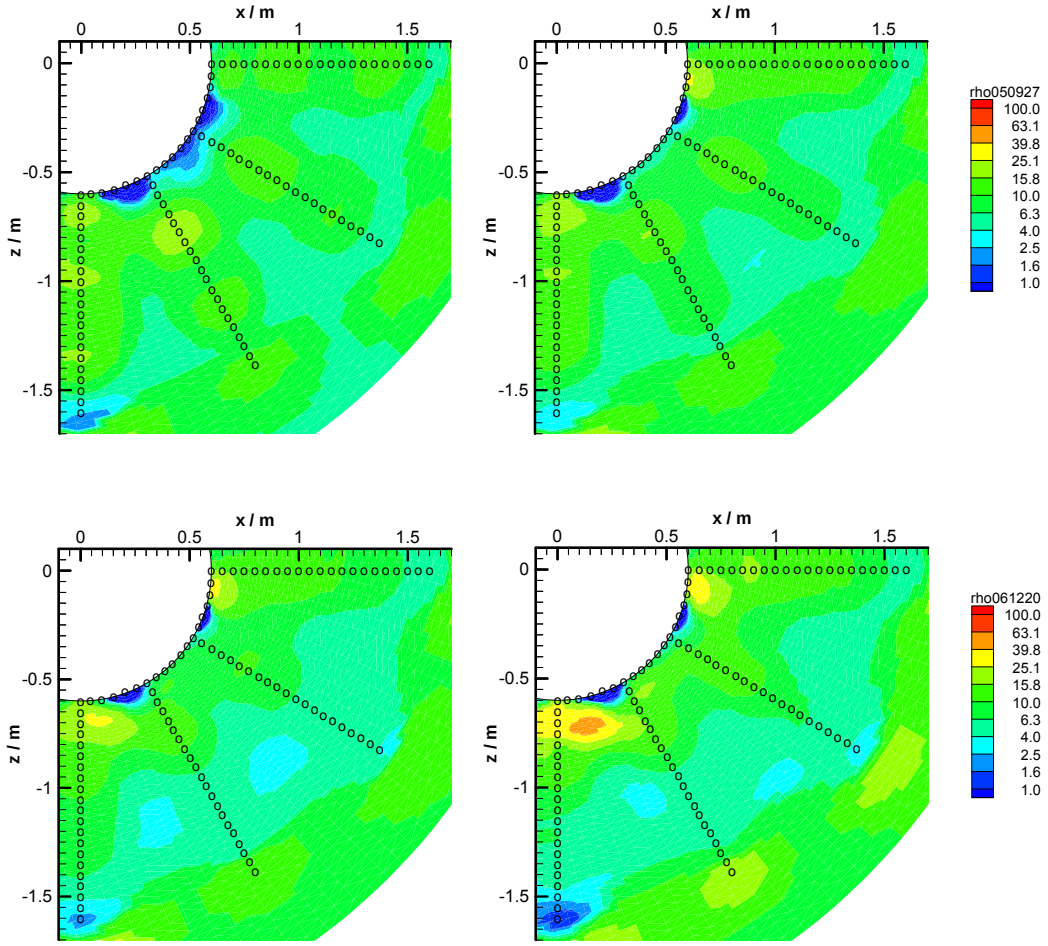

Figure 2-5 Resistivity tomograms of July 31, 2005 (upper left), September 27, 2005 (upper right), January 31, 2006 (lower left), and December 20, 2006 (lower right)

The desaturation effect and the extent of the desaturated zone become more visible when the relative change of the resistivity rather than the resistivity itself is plotted in the tomograms. This has been done in Figure 2-6 where the resistivity distributions of July 2005, December 2005 June 2006, and December 2006 are divided by the respective resistivity distribution of June 2005. The evolution of a desaturated zone of 30 cm width is clearly visible. The resistivity increase by a factor of 5 represents a desaturation in this zone down below 50 %.

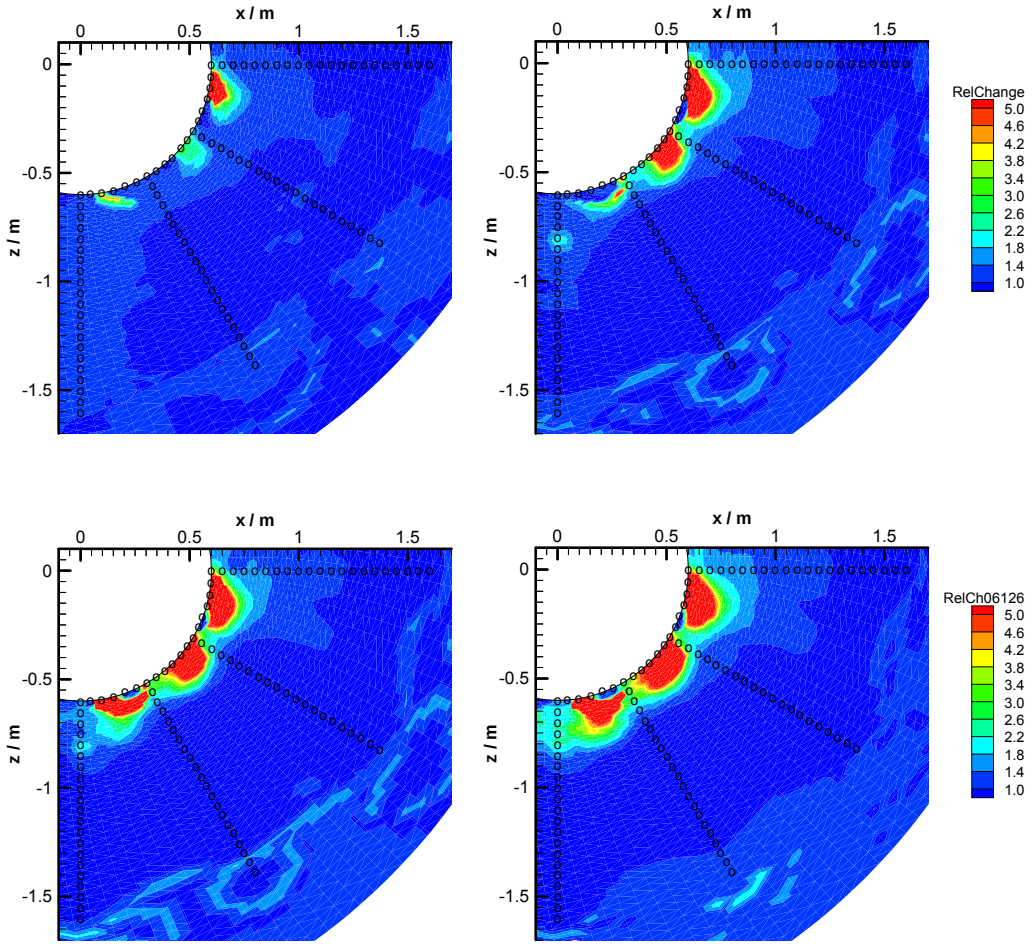

Figure 2-6 Relative change of resistivity during the desaturation phase with respect to the resistivity distribution on June 30, 2005 - July 31, 2005 (upper left), September 27, 2005 (upper right), January 31, 2006 (lower left), and December 20, 2006 (lower right). Dark blue = no change, red = increase by a factor of 5

2.5.4 Third resaturation phase

On December 21, 2006, the ventilation was stopped. In contrast to the earlier resaturation phases, no ventilation with humid air has been performed. Instead, resaturation proceeds by water migration from the undisturbed rock to the EDZ. Figure 2-7 shows the resistivity distribution and the relative change compared to the fully saturated state at the end of the second resaturation phase for the end of November 2007. Obviously, the EDZ is still not resaturated, although resaturation is proceeding.

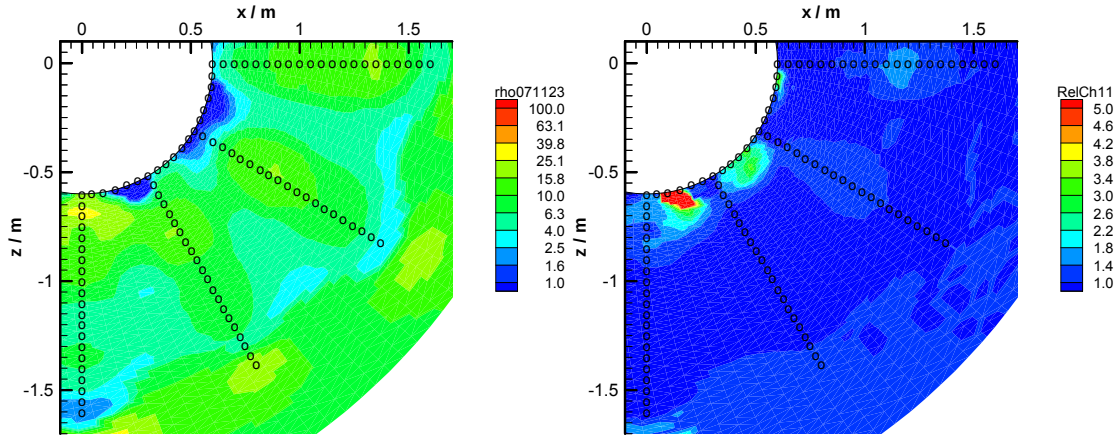

Figure 2-7 Resistivity tomogram of November 30, 2007 (left) and relative change of resistivity with respect to the resistivity distribution on June 30, 2005 (right). Dark blue = no change, red = increase by a factor of 5

3 Laboratory Investigations

In order to enable proper interpretation of the effects observed by the project partners during the in-situ ventilation experiment in addition to the geoelectric measurements performed by GRS, laboratory tests were performed by GRS on samples drilled from the VE test field area. The tests comprised the examination of water retention capacity, swelling pressure, and swelling / shrinking strains induced by moisture changes and response of hollow clay samples to humidity changes of the air ventilating the central boreholes. Some typical laboratory tests were also numerically simulated by hydro-mechanically coupled calculations with CODE_BRIGHT with regard to qualification of the code capabilities and to support the interpretation of observed effects.

3.1 Water retention

In highly-consolidated clay rocks, a very significant portion of the water content is adsorbed on clay mineral surfaces. The adsorbed water is so strongly bound that it may not be able to participate in advective transport under normally-encountered pressure gradients. However, the adsorbed water may be discharged thermodynamically from the pores at high external suction. In contrast, external water can also be taken up by unsaturated clays. The process of de- and re-hydration is controlled by the relationship between suction (s) and water content (w). The water retention curve of the Opalinus clay was determined on unconstraint samples placed in desiccators at different values of relative humidity (RH) or suction adjusted by means of salt solutions. The water contents reached in equilibrium are compared in Figure 3-1a with other data obtained by UPC /MUN 03/on constraint samples. It is evident that the water content decreases at high external suction and conversely increases at low suction. It is also obvious that the clay rock in unconstraint conditions can take up a large amount of water of up to 24 % at null suction, which is much higher than that of 8 % at volume constraint conditions. This finding confirms that most of the pore water in naturally-consolidated clay rocks is bound to clay minerals. Because of the negligible difference between the retention curves measured along the wetting and the drying paths, an average relationship between suction (s) and degree of water saturation (S) is established and described by the van Genuchten model (Fig. 3-1b):

$$S = \left[1 + \left(\frac{s}{p_o} \right)^{1/(1-\beta)} \right]^{-\beta} \qquad (3.1)$$

where the parameter p_o = 23 MPa and β = 0.4. It must be pointed out that the degree of water saturation was calculated by assuming a constant porosity of 16 %. This assumption may lead to some degree of uncertainty with the parameters. In fact, the sample porosity changes with suction due to its swelling and shrinking deformation.

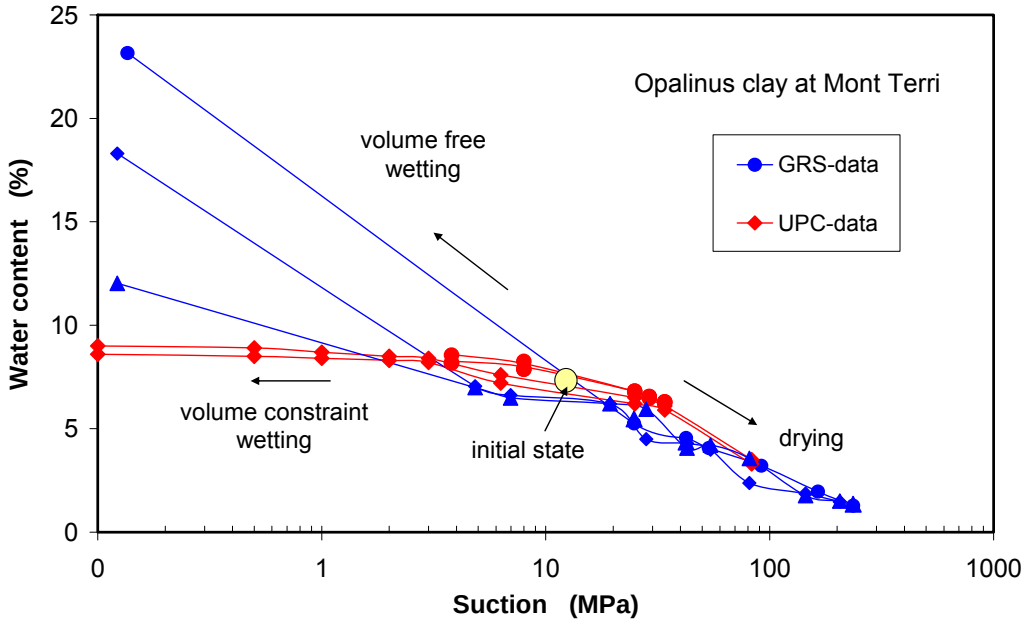

a: water content – suction

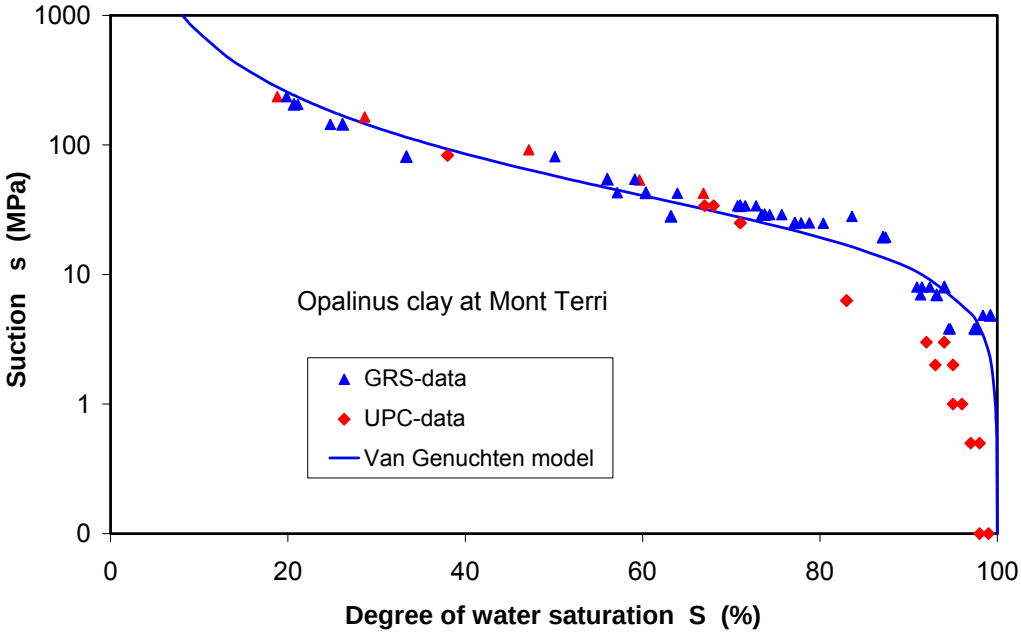

b: saturation degree - suction

Figure 3-1 Water retention curve of the Opalinus clay

3.2 Swelling / shrinking strains

In correspondence with the change in water content, the distance or pore space between solid particles changes too, resulting in swelling or shrinking strains. The magnitude of swelling and shrinkage is determined mainly by the clay content, the density, the amount of water uptake or release, and the confining stress. The swelling and shrinking behaviour of the Opalinus clay was investigated on unstressed samples which were first de-hydrated in a desiccator at a low humidity of RH = 23 % (s = 200 MPa) and then re-hydrated at a high humidity RH = 100 % (s = 0). Figure 3-2 shows an example of the tests. During the 2-months-drying-phase, the initially saturated sample (diameter D = 50 mm and length L = 47 mm) was de-saturated from an initial water content of w = 7.1 % to w = 1.7 % leading to a shrinkage or axial strain of up to ε_a = 1.2 %, a radial strain of ε_r = 0.2 %, and a volumetric strain of ε_v = 1.6 % (equal to porosity reduction). During the following wetting phase, the water content increased rapidly and the saturated state was recovered again within 15 days. After that, the water uptake rate kept nearly constant at 0.024 %/d. Over 6 months of re-hydration, the water content reached a high value of 10.5 %. With the water uptake, the sample expanded rapidly to its initial volume again in the first 10 days. Subsequently, a quasi-linear, large volume increase of ε_v = 11.2 % (ε_a = 7.5 %, ε_r = 1.8 %) was observed over 6 months. At that point, the sample broke down along a bedding plane

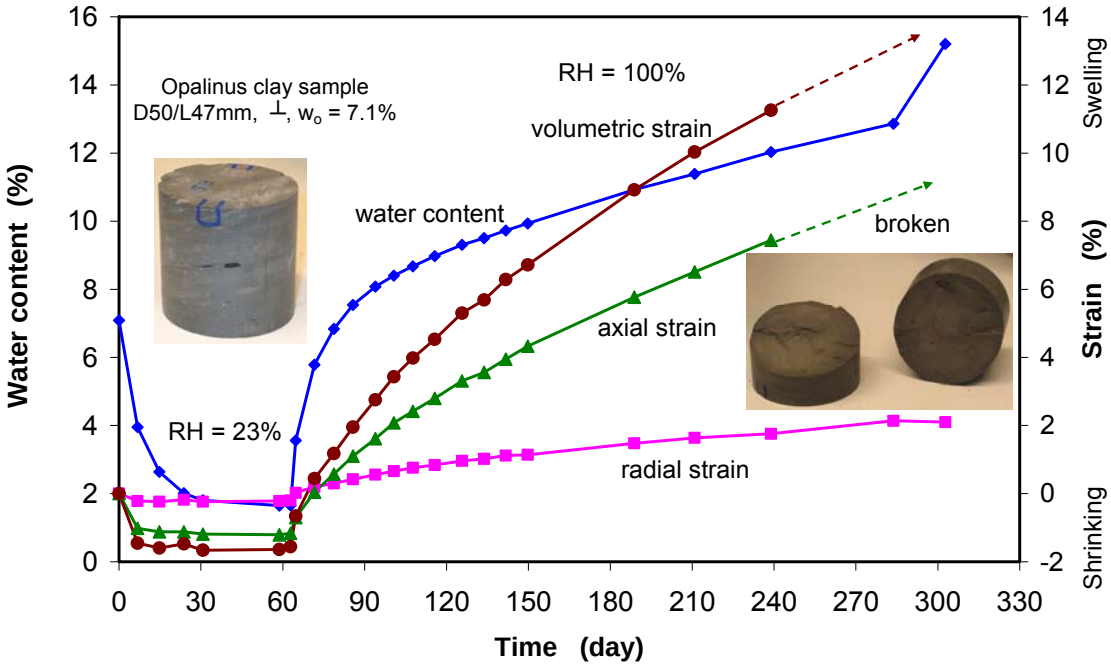

Figure 3-2 Swelling and shrinking behaviour of an unstressed Opalinus clay sample

perpendicular to the sample axis. Moreover, the separated pieces of the sample expanded further with water uptake. If wetting continued, more expansion of the clay rock could be expected. By contrast, free shrinkage is limited below 2 % after sufficient drying. Similar swelling / shrinking behaviour was also observed on samples of the Callovo-Oxfordian argillite. Additionally, the high swelling capacity of the clay rocks is confirmed by previous tests on samples at high confining stresses of up to 18 MPa /ZHA 04/07a/b). The anisotropy of the swelling and shrinking behaviour observed on the Opalinus clay is a typical character of argillaceous rocks, also as observed on the Tournemire shale /VAL 04/ and the Callovo-Oxfordian argillite /PHA 07/.

3.3 Swelling pressure

The swelling pressure of the Opalinus clay was examined using a newly developed test method /ZHA 04/. Figure 3-3 illustrates one test on a sample of D = 40 mm and L= 50 mm. The sample was first dried in room air. It was loaded to 2.5 MPa at laterally unconstraint conditions and then axially fixed. The sample was re-saturated by pumping water vapour into it. During this re-saturation phase of one month, the axial stress was monitored. The measurement shows that the axial stress increased with re-hydration and reached a maximum of 5.5 MPa at 95 % relative humidity. This value is very close to the major lithostatic stress of 6 – 7 MPa at Mont Terri /BOS 03/. A similar test result was found on a Callovo-Oxfordian argillite sample at a higher axial swelling pressure of ~11 MPa due to wetting at RH = 100 %. This pressure is almost equal to the overburden stress at the Bure site of ~12 MPa at the sampling depth of 455 m /ZHA 04/07b/. These test findings imply that interparticle water-films adsorbed in clay rocks are capable of carrying the lithostatic stress. Additionally, it is also interesting to note that the swelling pressure σ_a was built up in the fixed axial direction without any lateral confinement (σ_r = 0). This means that the pressure acting in the water-films is probably not a scalar quantity and should be represented by a second-rank tensor /HOR 96/, /ROD 99/.

3.4 Strength

Stiffness and strength of clay rocks strongly depend on water content. This issue was beyond the scope of this project, but has been investigated in the frame of other GRS projects. In order to enhance the understanding of the ventilation impact on the stability

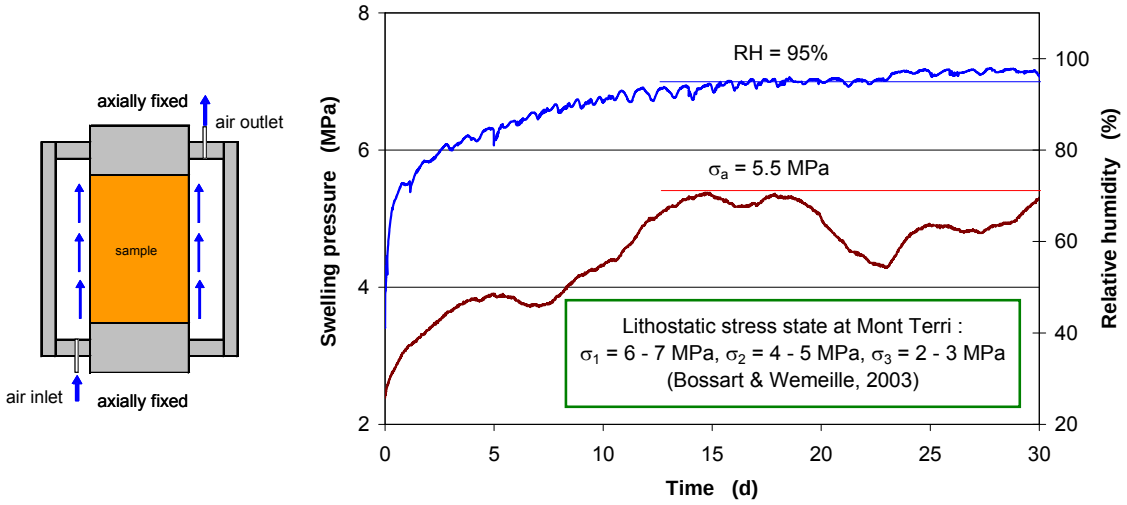

Figure 3-3 Axial swelling pressure measured on an Opalinus clay sample

of the EDZ around underground openings in clay rocks, some relevant test results reported by /ZHA 04/ and /BLU 05/ are briefly presented here. Figure 3-4a compares the uniaxial stress / strain curves of a saturated and an air-dried sample of the Callovo-Oxfordian argillite. Both failure strength and strain being reached at the air-dried sample are about two times higher than at the saturated sample. The dependence of strength on water content is presented in Figure 3-4b showing the data obtained on both the Opalinus clay and the Callovo-Oxfordian argillite at a confining stress of 10 MPa. The strength increase in dry conditions indicates that ventilation with dry air may enhance the self-support capability of the clay rocks around openings even despite some fissures induced by de-saturation.

3.5 Ventilation tests

In order to support the in situ VE experiment, laboratory ventilation tests were conducted on normal and large hollow clay samples by ventilating air through a central borehole under controlled conditions similar to the conditions in situ. The main objective of the tests was to investigate the hydro-mechanical response of the clay samples to changes in air humidity.

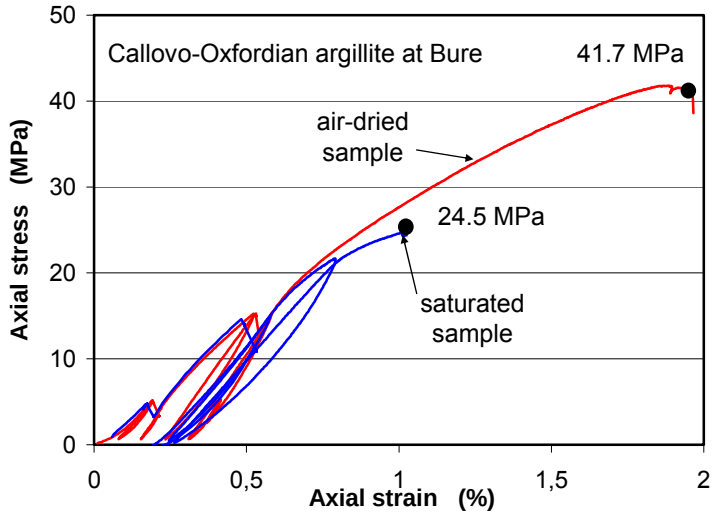

a: uniaxial stress / strain curves (after /ZHA 04/)

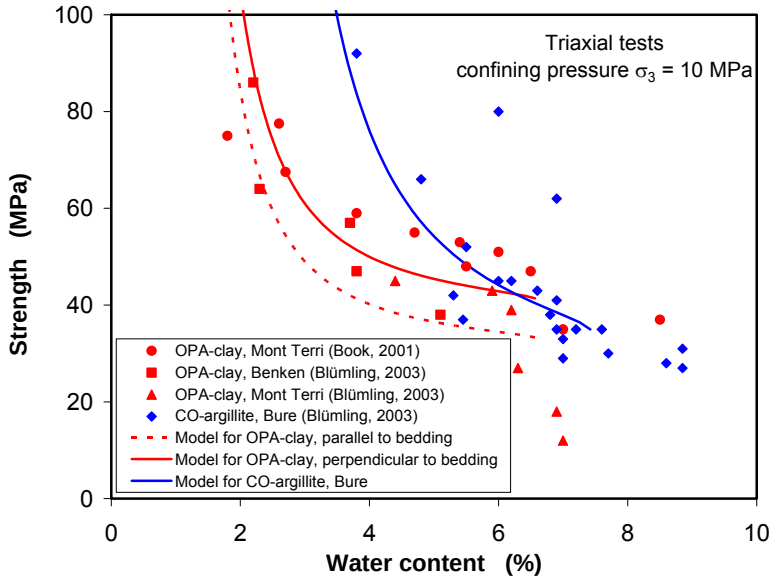

b: strength in dependence of water content (after Blümling et al. /BLU 05/)

Figure 3-4 Effects of water content on the stress / strain behaviour and the strength of clay rocks

3.5.1 Normal samples

The first VE tests were carried out on normally-sized clay samples of the Opalinus clay and the Callovo-Oxfordian argillite. Figure 3-5 presents schematically the test system for the ventilation of two Opalinus clay samples with central boreholes. During the long-term storage, the samples were sealed in vacuum-tight foils, but without confining pressure. Therefore, fissures developed along the bedding planes showing an inclination of ~40° to the sample axis. But the reasons for fissuring are not completely

understood. Sample A (D/d/L = 100/20/100 mm) was loaded in a triaxial cell and then de- and re-saturated by pumping air through the borehole. The relative humidity of the air was regulated by mixing dry air and water vapour in a desired ratio with two air pumps. Because the water content of the loaded sample could not be directly measured during the test, a second sample B (D/d/L = 100/20/120 mm) was used, which was inserted in the same ventilation system, but without external confining pressure. From sample A, the air flow continued through the borehole of sample B. During the test, the following parameters were controlled and/or measured: axial stress (σ_a) / strain (ε_a) and outer radial stress (σ_r) / strain (ε_r) on sample A, water content (w) on sample B, and temperature (T), flow rate (Q), and relative humidity (RH) in the ventilation system.

The ventilation was carried out at room temperature of ~20 °C by ventilating air at a controlled rate of 0.2 l/min and with different values of relative humidity RH ≈ 99 %, 60 %, 23 %, and 90 %. Each phase lasted 20 to 30 days. Figure 3-5b shows the applied axial and radial stress as well as the relative humidity of the air, whereas the response of both deformation of sample A and water content of sample B is illustrated in Figure 3-5c. Sample A was first loaded up to a confining stress of 3.5 MPa. During the first ventilation phase at a high humidity value of 99 %, no significant changes in water content and axial / radial strain appeared because of the high initial saturation in the samples. Subsequently, the axial stress was increased to 6.7 MPa resulting in axial compaction and radial extension. After fixing the load piston ($\Delta\varepsilon_a = 0$), the axial stress decreased with time to the same level of 3.5 MPa as the lateral stress. The subsequent drying phase at ~60 % humidity led to a reduction in water content and a compaction. Further water release and compaction was caused by lowering the air humidity to ~23 %. Totally, the two drying phases over 1.5 months caused a water loss of about 3 % and a volumetric compaction of 0.8 %. After increasing the air humidity to ~90 % again, the samples were re-saturated and expanded up to 0.3 % over one month.

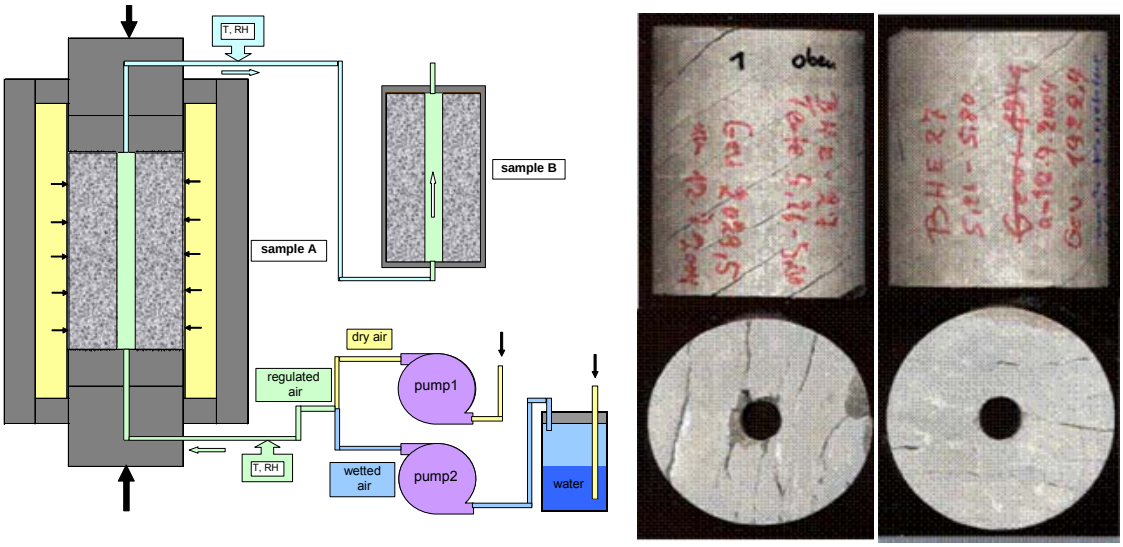

a. Test system Sample A Sample B

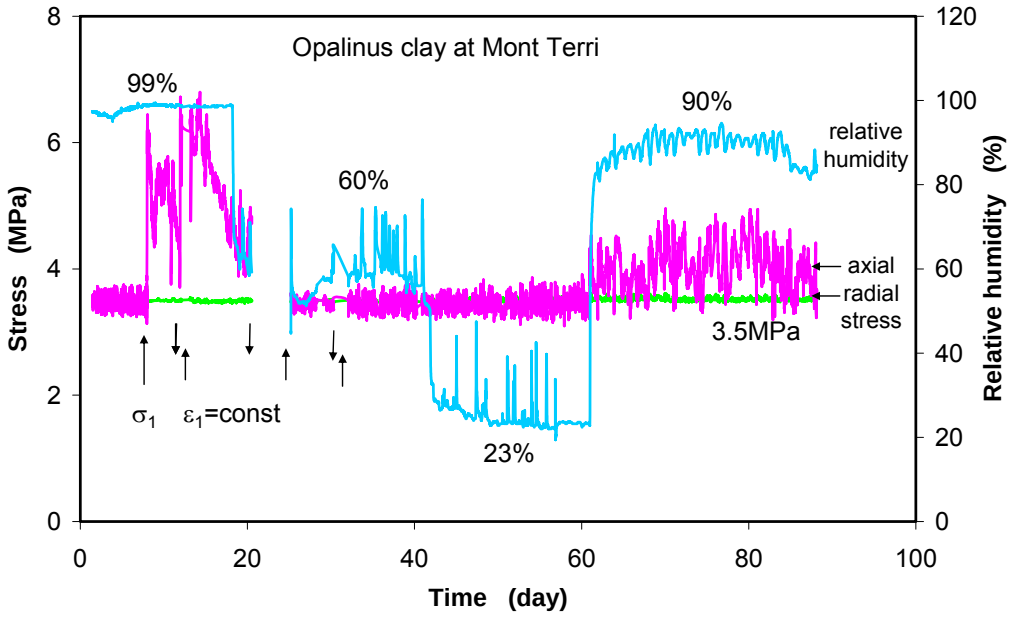

b: Applied stress and relative humidity

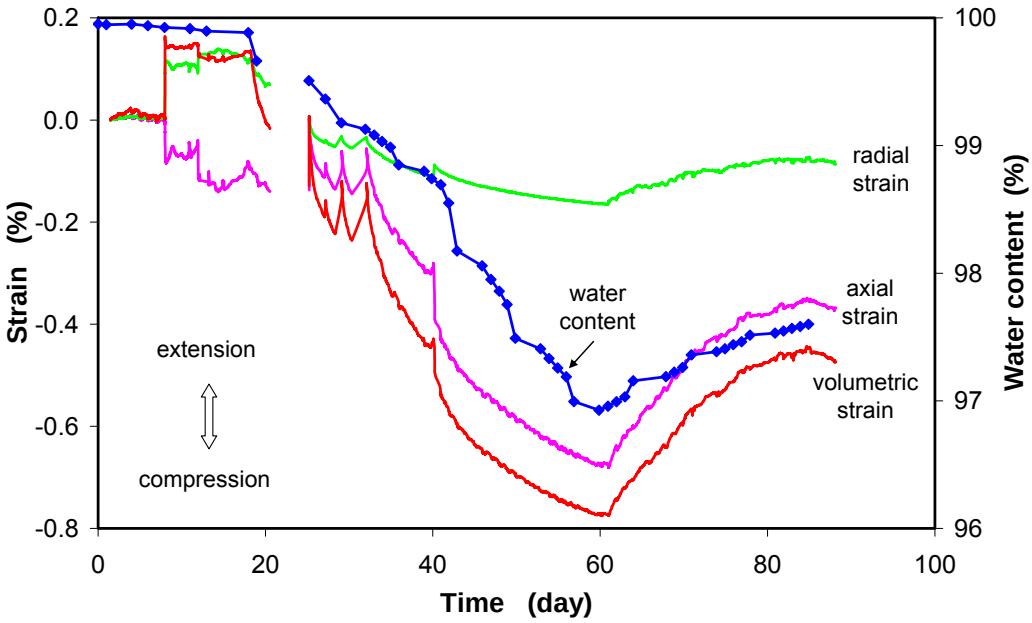

c: Responses of strain and water content

Figure 3-5 Ventilation test on normal hollow samples of the Opalinus clay

3.5.2 Large samples

Based on the experience from the ventilation tests on normal hollow samples and pre-operational calculations, large-scale ventilation tests were carried out on big cores of the Opalinus clay and the Callovo-Oxfordian argillite. One test was performed on a large Opalinus clay core of 260 mm diameter and 465 mm length, which had been drilled from a borehole of the SB experiment at the URL Mont Terri. Immediately after drilling, the core was sealed vacuum-tight in aluminium foil, then covered by a rubber jacket, and finally mechanically confined by pressing plastic tubes over the jacket using stretching bands. This confined core was stored in a air-conditioned room at 22°C over more than one year. A short time before starting the test, a water content of 6.8 % was measured at 105°C over 48 hours. A central borehole of 55 mm diameter was drilled axially through the sample. Figure 3-6 shows schematically the test assembly. The sample was not stressed, but sealed against ambient air. The ventilation was conducted with two drying / wetting cycles by changing the humidity of the air ventilating the borehole at a temperature of 25±0.5°C. The air flow is controlled at a rate of 0.2 l/min. A dilatometer was installed in the borehole allowing the registration of its deformation in four different directions of 0°/45°/90°/135°. During ventilation,

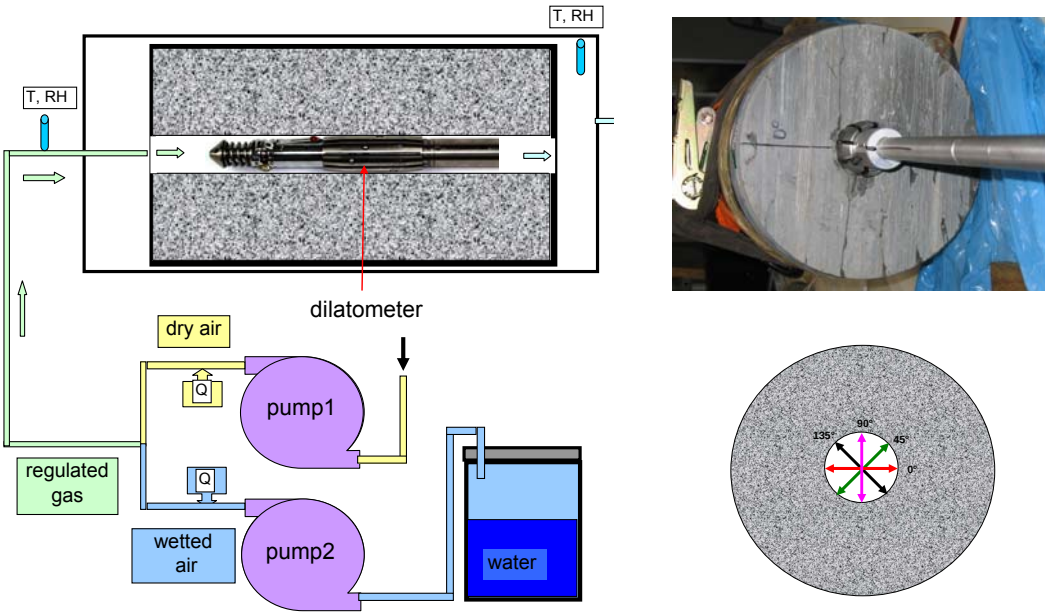

a: Ventilation test system

b: Large Opalinus clay sample (D/d/L=260/55/465mm) with sensors in four directions

Figure 3-6 Large-scale ventilation test on a large hollow Opalinus clay sample

temperature and relative humidity were monitored on both inlet and outlet sides as well as inside the borehole.

Figure 3-7 shows the evolution of borehole deformation in three directions of 0°/45°/90° in relation to the humidity change in the borehole during ventilation. Initially, a high relative humidity of 95 % was kept for 6 days. No significant borehole deformation was observed. By pumping room air with a low RH value of ~50 % into the borehole, the sample was dried leading to a borehole divergence of up to 0.2 %. This deformation continued even over the first 15 days of the subsequent wetting phase. Following divergence, the borehole converged gradually with increasing humidity from 88 % to 90 % over 40 days. Depending on the drying and wetting rates, however, the convergence rates are clearly lower than the divergence rates. The second drying / wetting cycle by opening the borehole to the atmosphere for 40 days (RH ≈ 50 %) and by elevating the humidity to 80 % for another 40 days caused a progressive divergence and convergence of the borehole again. The deformation curves in the stated test directions are quite parallel. The discrepancy between the strain-time curves in 0°-direction and 45°- / 90°-direction might depend on different local conditions at the measuring positions. A clear anisotropic behaviour could not be identified. The test

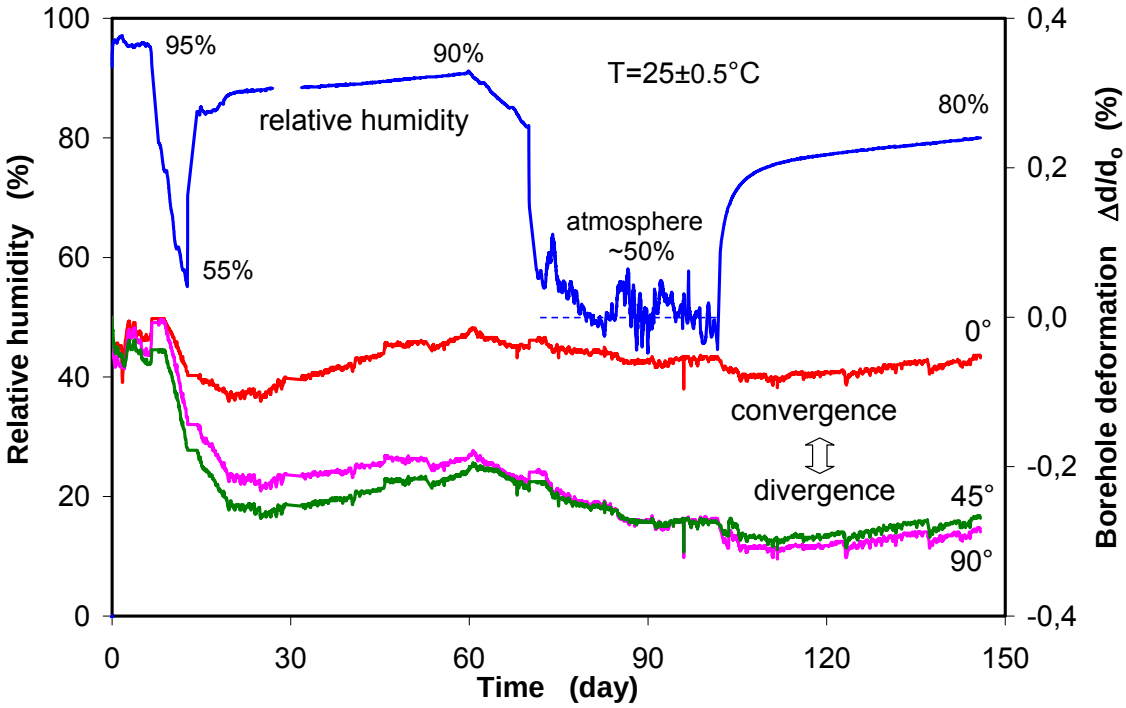

Figure 3-7 Evolution of borehole deformation during ventilation

observations suggest that boreholes in clay rocks converge with increasing humidity of the ventilated air and diverge vice versa.

4 Modelling work

The modelling work included the determination of parameters, pre-operational calculations for the test design, and the simulation of the laboratory ventilation tests using CODE-BRIGHT /UPC 04/. The results are documented in NF-RRO deliverables D3.3.4a/b /ZHA 07b/. A typical simulation of the ventilation test mentioned in section 3.5.1 is presented here.

Considering the processes observed on Opalinus clay samples during ventilation, the test is simulated by hydro-mechanically coupled calculations, in which a set of balance equations of energy, solid mass, water mass, air mass, and stress equilibrium is solved. The samples are considered as a homogeneous and isotropic porous medium with a grain density of 2.71 g/cm^3, a dry density of 2.34 g/cm^3, a porosity of 16 %, a water content of 6.85 % and an intrinsic permeability of $2 \cdot 10^{-20}$ m^2. Water de- and re-saturation of the samples during ventilation is assumed to be dominated by the relationship of water saturation with suction established in section 5.3.1 (Fig. 3-1). In the modelling, however, a set of constitutive laws is applied for the description of the hydraulic process including Darcy's law for liquid/gas advection, Fick's law for vapour diffusion, and Kelvin's law for liquid/gas-phase change. Air solution in the liquid phase is not taken into account. The deformation of the clay rock is considered to consist of two parts: (a) elasto-plastic strain produced by mechanical loading and (b) non-linear swelling/shrinking strain induced by moisture change. The mechanical behaviour is approached by an elasto-plastic model. The main features of the hydro-mechanical models and the associated parameters for the Opalinus clay are given in /ZHA 07c/ and in the literature /UPC 04/.

Figure 4-1 shows the 2D axisymmetric model for the hollow sample of D/d/L = 100/20/100 mm and the simplified test conditions. With a saturation degree of 99 % corresponding to a suction of 1 MPa, the initial state of the sample was not fully saturated. The ventilation is simulated by applying relative humidity values of RH = 99 % (s = 1 MPa), RH = 60 % (s = 70 MPa), RH = 23 % (s = 200 MPa) and RH = 90 % (s = 14 MPa) to the borehole wall. Along the borehole wall, the sensitivity of the turbulence coefficient of the airflow has been studied.

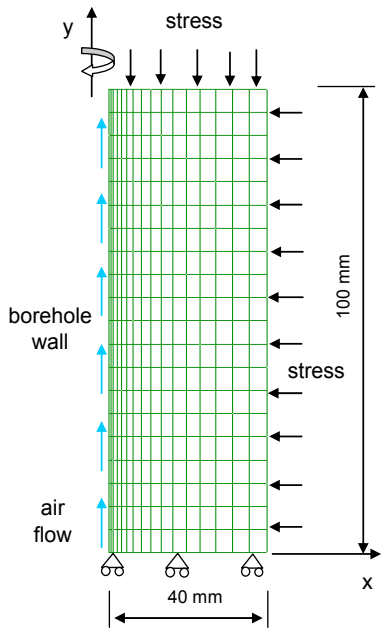

a: Finite element mesh

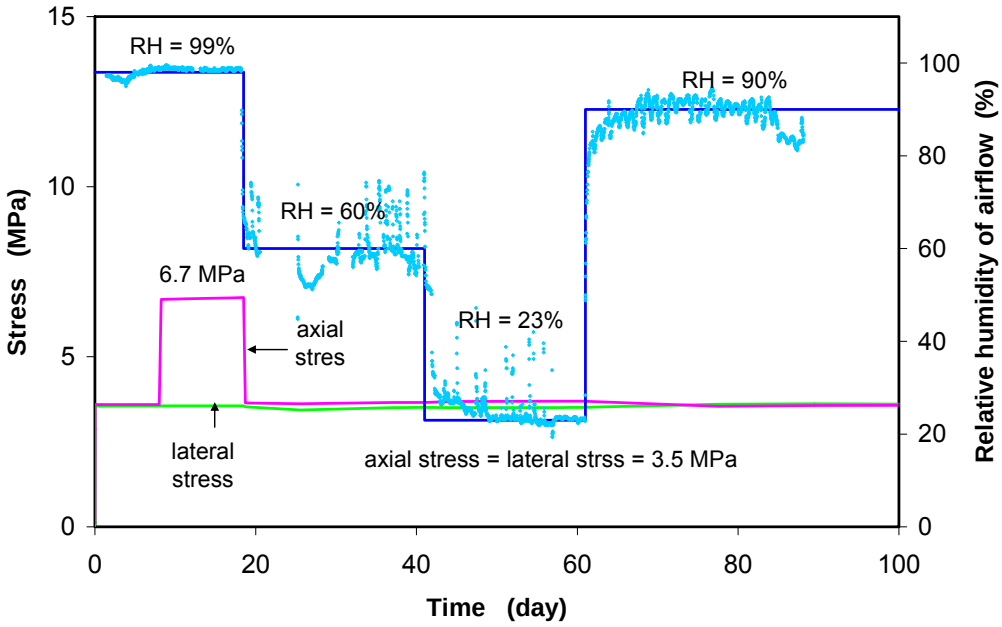

b: Applied stress and relative humidity

Figure 4-1 Numerical model and boundary conditions

In Figure 4-2, the modelling results are compared with the measured water content and strain data. As shown in Fig. 4-2a, the turbulence coefficient of ß = $5 \cdot 10^{-3}$ m/s for the airflow through the borehole fits the test data pretty well. Using the optimised parameters, the deformation of the stressed sample due to ventilation is calculated (Fig. 4-2b). Generally, the strain response to drying and wetting is reasonably

represented by the model. However, neither the observed relatively high sensibility of axial strain to moisture changes nor the large radial strain which was caused by increasing axial stress to 6.7 MPa could be reproduced quantitatively by the model. This may be due to the pre-existing fractures in the sample which are more sensible to load and moisture changes.

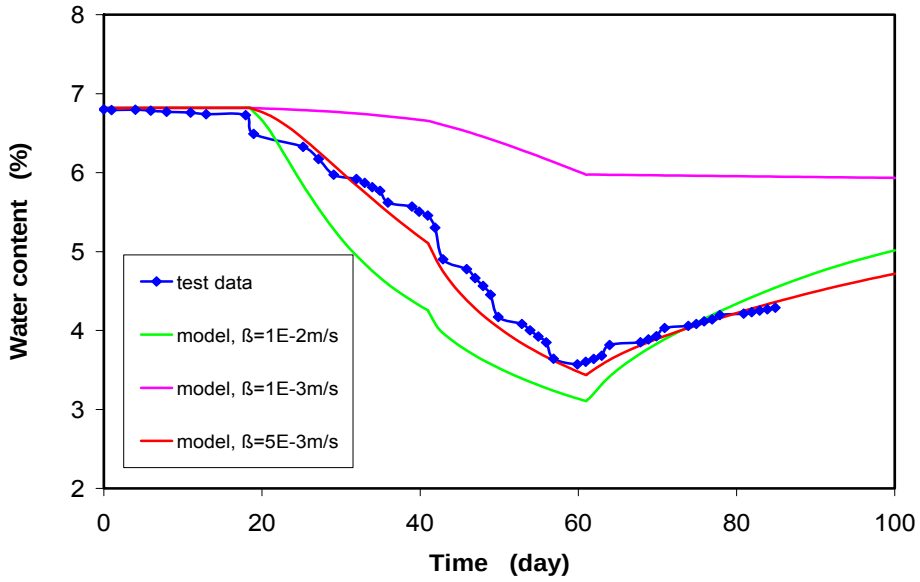

a: Water content

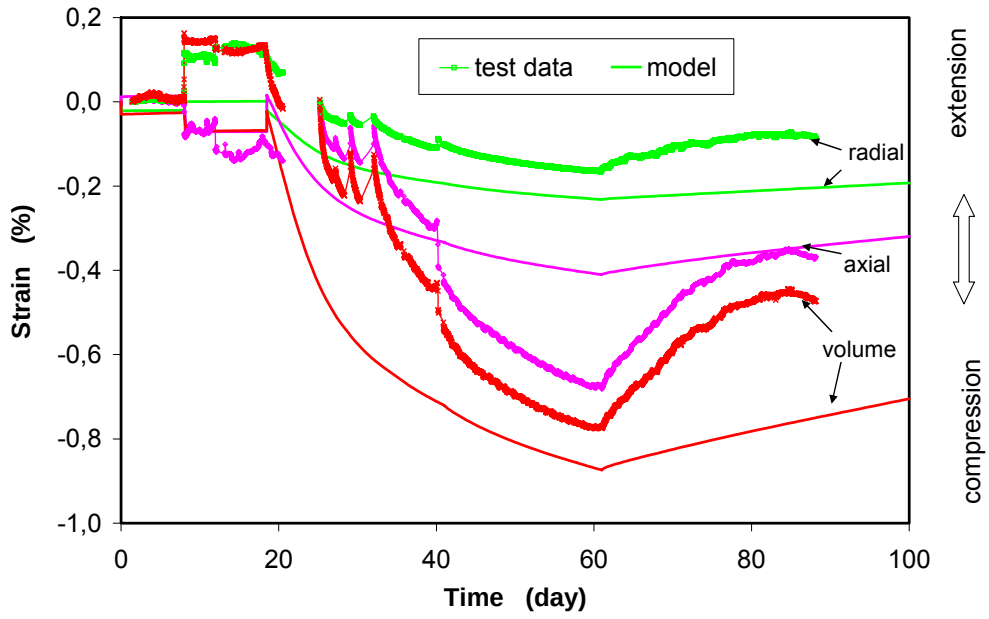

b: Deformation

Figure 4-2 Modelling results of water content and strain evolution during the ventilation test in comparison with the test data

5 Conclusions

The results of the geoelectric measurements performed in the second phase of the Mont Terri Ventilation Test can be summarized as follows:

- Geoelectric tomography has been found suitable for monitoring ventilation-induced saturation changes in the Opalinus clay.
- During ventilaton with dry air a desaturation down to below 50 % could be detected in both desaturation cycles. The desaturated zone extends less than 0.5 m into the rock around the microtunnel.
- During the second resaturation phase, ventilation with humid air led to quick resaturation at the tunnel surface, while resaturation of the rock mass took months. The still ongoing third resaturation phase seems to imply that resaturation of the rock mass may take years with no air circulation in the tunnel.

The laboratory investigations on the Opalinus clay included the determination of water retention capacity, swelling pressure, free swelling / shrinking strains induced by moisture changes, and response of normal and large hollow clay samples to the ventilation of the central boreholes at different air humidity values. The main conclusions can be drawn as follows:

- The Opalinus clay has a high water absorption capacity. The amount of water uptake in unconstraint conditions is much higher than the water content in the naturally confined state, indicating that the pore water in the natural clay rock is predominantly bound on clay minerals.
- The swelling pressure induced by wetting with vapour is very close to the major lithostatic stress at the sampling location, suggesting that interparticle water-films in the consolidated clay are capable of carrying the lithostatic stress.
- Water uptake from vapour causes a large free expansion of up to 12 % over 8 months and even a breakdown along bedding planes.
- Release of pore water reduces the inner swelling pressure and causes collapse of the pore structure. The free shrinkage is limited to 2 %.
- Boreholes in clay samples converge with increasing humidity of the ventilated air and diverge vice versa.

The laboratory ventilation tests were also numerically simulated by hydro-mechanically coupled calculations with CODE_BRIGHT. The hydro-mechanical processes in the clay samples can be reasonably represented by modelling, but some phenomena which were observed in the tests require further model improvement, especially the pronounced anisotropy of swelling pressure and strain, the fracturing induced by moisture changes, and the continuing expansion even after full saturation of the samples.

6 References

/BLU 05/ Blümling, P., Bernier, F., Lebon, P., Martin, C. D. (2005): The Excavation-Damaged Zone in Clay Formations – Time dependent Behaviour and Influence on Performance Assessment. 2nd International Meeting of Clays in Natural & Engineered Barriers for Radioactive Waste Confinement, Tours, March 14-18, 2005.

/BOS 03/ Bossart, P., Wermeille, S. (2003): The Stress Field in the Mont Terri Region - Data Compilation. In: Heitzmann, P. & Tripet, J.-P. (ed.): Mont Terri Project – Geology, Paleohydrology and Stress Field of the Mont Terri Region – Reports of Federal Office for Water and Geology (FOWG), Geology Series 4, 2003.

/FEC 01/ Fechner, T. (2001) SensInv2D-Manual, Geotomographie, Neuwied.

/HOR 96/ Horseman, S. T., Higgo, J. J. W., Alexander, J., Harrington, J. F. (1996): Water, Gas and Solute Movement through Argillaceous Media. Report CC-96/1, 1996.

/KEM 95/ Kemna, A. (1995): Tomographische Inversion des spezifischen Widerstandes in der Geoelektrik, Master Thesis, Universität Köln.

/MUN 02/ Munoz, J. J., Lioret, A., Alonso, E. (2003): Characterization of hydraulic properties under saturated and non-saturated conditions, VE-Experiment, 2003.

/PHA 07/ Pham, Q.T., Vales, F., Malinsky, L., Nguyen Minh, D., Gharbi, H. (2007): Effects of desaturation-resaturation on mudstone, Physics and Chemistry of the Earth, Vol. 32, 8-14, 2007, p. 646-655.

/ROD 99/ Rodwell, W. R., Harris, A. W., Horseman, S. T. et al. (1999): Gas Migration and Two-Phase Flow through Engineered and Geological Barriers for a Deep Repository for Radioactive Waste. EC/NEA Status Report, EUR 19122 EN.

/ROT 04/ Rothfuchs, T., Hartwig, L., Hellwald, K., Komischke, M., Miehe, R., Wieczorek, K. (2004): Ventilation Test at Mont Terri: Geoelectric Monitoring of Opalinus Clay Desaturation, Gesellschaft für Anlagen- und Reaktorsicherheit mbH, GRS-207.

/UPC 04/ UPC (2004): CODE-BRIGHT, A 3-D program for thermo-hydro-mechanical analysis in geological media.

/VAL 04/ Vales, F., Nguyen Minh, D., Gharbi, H., Rejeb, A. (2004): Experimental study of the influence of the degree of saturation on physical and mechanical properties in Tournemire shale (France), Applied Clay Science, 26 (2004), p. 197-207.

/ZHA 04/ Zhang, C.-L., Rothfuchs, T. (2004): Experimental Study of Hydromechanical Behaviour of the Callovo-Oxfordian Argillites, Applied Clay Science, 26 (2004), p. 325-336.

/ZHA 07a/ Zhang, C.-L., Rothfuchs, T., Su, K., Hoteit, N. (2007): Experimental Study of the thermo-hydro-mechanical behaviour of indurated Clays, Physics and Chemistry of the Earth, Vol. 32, 8-14, 2007, p. 957-965.

/ZHA 07b/ Zhang, C.-L., Rothfuchs, T. (2007): Moisture Effects on Argillaceous Rocks. In: Proceedings 2nd International Conference of Mechanics of Unsaturated Soils (ed. T. Schanz), Springer Proceedings in Physics 112, p. 319-326.

/ZHA 07c/ Zhang, C.-L., Rothfuchs, T., (2007): GRS' Deliverables in the frame of NF-PRO-RTDC4-WP4.3,
D 4.3.4a: Determination of material parameters for the Opalinus clay, December 2004;
D 4.3.4b: Scoping calculations for laboratory ventilation tests and test plan, June 2005;
D 4.3.11: Report on instrument layout and testing, June 2005;
D 4.3.14: Results of laboratory ventilation tests on large clay samples, June 2007.

7 List of Figures

Gesellschaft für Anlagen- und Reaktorsicherheit (GRS) mbH

Schwertnergasse 1
50667 Köln
Telefon +49 221 2068-0
Telefax +49 221 2068-888

Forschungsinstitute
85748 Garching b. München
Telefon +49 89 32004-0
Telefax +49 89 32004-300

Kurfürstendamm 200
10719 Berlin
Telefon +49 30 88589-0
Telefax +49 30 88589-111

Theodor-Heuss-Straße 4
38122 Braunschweig
Telefon +49 531 8012-0
Telefax +49 531 8012-200

www.grs.de

ISBN 978-3-939355-09-0